

Theoretical Study and Luminescence Properties of the Cyclic $\text{Cu}_3(\text{dppm})_3\text{OH}^{2+}$ Cluster. The First Luminescent Cluster Host at Room Temperature

Réjean Provencher and Pierre D. Harvey*

Département de chimie, Université de Sherbrooke, Sherbrooke, Québec, Canada J1K 2R1

Received June 29, 1995[⊗]

The $[\text{Cu}_3(\text{dppm})_3\text{OH}](\text{BF}_4)_2$ cyclic cluster host is found to be luminescent at 298 K ($\lambda_{\text{max}} = 540 \text{ nm}$; $\tau_e = 89 \pm 9 \mu\text{s}$; $\Phi_e = 0.14 \pm 0.01$) in degassed ethanol solutions and at 77 K ($\lambda_{\text{max}} = 480 \text{ nm}$; $\tau_e = 170 \pm 40 \mu\text{s}$; $\Phi = 0.73 \pm 0.07$) also in ethanol. The nature of the lowest energy excited states has been addressed theoretically using density functional theory and experimentally using UV–visible, luminescence, and polarized luminescence spectroscopy and is found to be 1A_2 arising from the $\dots(18e)^4(7a_2)^1(13a_1)^1$ electronic configuration. The excited state geometry optimization for the model $\text{Cu}_3(\text{PH}_3)_3\text{OH}^{2+}$ compound in its T_1 state (3A_2) has been performed using density functional theory and compared to its ground state structure. The $\text{Cu}\cdots\text{Cu}$ bond length is expected to decrease greatly in the excited state (calculated $\Delta Q \sim 0.47 \text{ \AA}$), in agreement with the d^{10} electronic configuration. The perturbation of the photophysical properties by the addition of two guest carboxylate anions has been investigated. From the Stern–Volmer plots, the quenching constants, k_q , are 1.65×10^8 and $5.10 \times 10^8 \text{ M}^{-1} \text{ s}^{-1}$ for acetate and 4-aminobenzoate, respectively, which are also proportional to the relative binding strengths of the substrates with $\text{Cu}_3(\text{dppm})_3\text{OH}^{2+}$ (i.e., acetate < 4-aminobenzoate).

Introduction

The Cu^I cluster complexes have been the topic of numerous theoretical and spectroscopic studies regarding the nature of the lowest energy luminescent excited states and the presence of $\text{Cu}^I\cdots\text{Cu}^I$ interactions.¹ The Cu^I species belong to a larger family of compounds where the electronic configuration is d^{10} (Cu^I , Ag^I , Au^I , Ni^0 , Pd^0 , Pt^0), which again also exhibit rich photophysical properties.^{2–4} Recently our group has been interested in low valent trinuclear cyclic clusters of the type

$\text{M}_3(\text{dppm})_3\text{CO}^{2+}$ ($\text{M} = \text{Pd}, \text{Pt}$; $\text{dppm} = ((\text{C}_6\text{H}_5)_2\text{P})\text{CH}_2$) in relation to the presence of guest–host interactions, both in the ground and excited states.⁵ These complexes exhibit a hydrophobic cavity located above the unsaturated M_3 center, which is formed by six dppm phenyl groups arranged like a “picket fence”. The $\text{M}_3(\text{dppm})_3\text{CO}^{2+}$ ground state structure exhibits a formal $\text{M}–\text{M}$ single bond and a cavity size of $\sim 2–3 \text{ \AA}$ diameter.⁶ On the other hand, theoretical and experimental considerations indicate that both the $\text{M}–\text{M}$ bond and cavity size increase from the ground to the lowest energy excited states.^{5b,7} Cyclic trimetallic $\text{M}_3(\text{dppm})_3\text{X}_n$ compounds exhibiting weak $\text{M}\cdots\text{M}$ interactions exist such as in the saturated $\text{Ag}_3(\text{dppm})_3\text{Br}_2^+$ ⁸ and $\text{Cu}_3(\text{dppm})_3\text{Cl}_2^+$ clusters.⁹ Many years ago Ho and Bau reported the only example of a $d^{10}–d^{10}–d^{10}$ complex exhibiting an unsaturated face.¹⁰ The three latter clusters have been proposed as structural models for the lowest energy excited state $\text{M}_3(\text{dppm})_3\text{CO}^{2+}$ ($\text{M} = \text{Pd}, \text{Pt}$) species.^{5b}

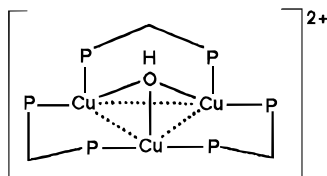
We now wish to report the spectroscopic and photophysical properties of the “strongly” luminescent $\text{Cu}_3(\text{dppm})_3\text{OH}^{2+}$ complex. This compound is found to be luminescent both in 298 and 77 K solutions and in the solid state. The molecular

*To whom correspondence should be addressed. Tel: (819) 821-7092. FAX: (819) 821-8017. e-mail: pharvey@structure.chimie.usherb.ca.

⊗ Abstract published in *Advance ACS Abstracts*, March 15, 1996.

- (1) (a) Lai, D. C.; Zink, J. I. *Inorg. Chem.* **1993**, 32, 2594. (b) Ryu, C. K.; Vitale, M.; Ford, P. C. *Inorg. Chem.* **1993**, 32, 869. (c) Ryu, C. K.; Kyle, K. R.; Ford, P. C. *Inorg. Chem.* **1991**, 30, 3982. (d) Kyle, K. R.; Ryu, C. K.; Ford, P. C. *J. Am. Chem. Soc.* **1991**, 113, 2954. (e) Kyle, K. R.; Palke, W. E.; Ford, P. C. *Coord. Chem. Rev.* **1990**, 95, 35. (f) Henary, M.; Zink, J. I. *J. Am. Chem. Soc.* **1989**, 111, 7404.
- (2) (a) Rath, N. P.; Holt, E. M.; Tanimura, K. *J. Chem. Soc., Dalton Trans.* **1986**, 2303. (b) Volger, A.; Kunkely, H. *J. Am. Chem. Soc.* **1986**, 108, 7211. (c) Rath, N. P.; Holt, E. M.; Tanimura, *Inorg. Chem.* **1985**, 24, 3934. (d) Hardt, H. D.; Stroll, H.-J. *Z. Anorg. Allg. Chem.* **1981**, 480, 199. (e) Eitel, E.; Oelkrug, D.; Hiller, W.; Strähle, J. *Z. Naturforsch.* **1980**, 35B, 1247.
- (3) (a) McCleskey, T. M.; Gray, H. B. *Inorg. Chem.* **1992**, 31, 1733. (b) Assefa, Z.; Destefano, F.; Garepapaghi, M. A.; LaCasce, J. H., Jr.; Ouellete, S.; Corson, M. R.; Nagle, J. K.; Patterson, M. H. *Inorg. Chem.* **1991**, 30, 2862. (c) Balch, A. C.; Catalano, V. J.; Olmstead, M. M. *Inorg. Chem.* **1990**, 29, 585. (d) Che, C.-M.; Kwon, H.-L.; Yam, V. W.-W.; Cho, K.-C. *J. Chem. Soc., Chem. Commun.* **1989**, 885. (e) Sabin, F.; Ryu, C. K.; Volger, A.; Ford, P. C. *Inorg. Chem.* **1992**, 31, 1941. (f) Caspar, J. V. *J. Am. Chem. Soc.* **1985**, 107, 6718. (g) Khan, M. N. I.; Fackler, J. P., Jr.; King, C.; Wang, J. C.; Wang, S. *Inorg. Chem.* **1988**, 27, 1672. (h) Che, C. M.; Wong, W. T.; Lai, T.-F.; Kwong, H.-L. *J. Chem. Soc., Chem. Commun.* **1989**, 243. (i) Balch, A. L.; Nagle, J. K.; Oram, D. E.; Reedy, P. E., Jr. *J. Am. Chem. Soc.* **1988**, 110, 454. (j) Wang, S.; Fackler, J. P., Jr.; King, C.; Wang, J. C. *J. Am. Chem. Soc.* **1988**, 110, 3308.
- (4) (a) Harvey, P. D. *Inorg. Chem.* **1995**, 34, (b) Piché, D.; Harvey, P. D. *Can. J. Chem.* **1994**, 72, 705. (c) Harvey, P. D.; Gan, L. *Inorg. Chem.* **1990**, 30, 3239. (d) Perreault, D.; Drouin, M.; Michel, A.; Harvey, P. D. *Inorg. Chem.* **1991**, 30, 2. (e) Hubig, S. M.; Drouin, M.; Michel, A.; Harvey, P. D. *Inorg. Chem.* **1992**, 31, 3688. (f) Harvey, P. D.; Gray, H. B. *Polyhedron* **1990**, 9, 1949. (g) Harvey, P. D.; Adar, F.; Gray, H. B. *J. Am. Chem. Soc.* **1989**, 111, 1312. (h) Harvey, P. D.; Gray, H. B. *J. Am. Chem. Soc.* **1988**, 110, 21245. (i) Harvey, P. D.; Schaefer, W. P.; Gray, H. B. *Inorg. Chem.* **1988**, 27, 1101.

- (5) (a) Harvey, P. D.; Crozet, M.; Aye, K. T. *Can. J. Chem.* **1995**, 73, 123. (b) Harvey, P. D.; Hubig, S.; Ziegler, T. *Inorg. Chem.* **1994**, 33, 3700. (c) Provencher, R.; Aye, K. T.; Drouin, M.; Gagnon, J.; Boudreault, N.; Harvey, P. D. *Inorg. Chem.* **1994**, 33, 3689. (d) Provencher, R.; Harvey, P. D. *Inorg. Chem.* **1993**, 32, 61.
- (6) Puddephatt, R. J.; Manojlovic-Muir, L.; Muir, K. W. *Polyhedron* **1990**, 9, 2767.
- (7) The molecular structures for $\text{Pd}_3(\text{dppm})_3\text{CO}^{2+}$ in the lowest energy 3E and 3A_2 states have been calculated using a program called AMOL and the density functional theory (ADF 113) and are in agreement with the findings in ref 5b. For instance, the ΔQ value for the emissive 3A_2 state in $\text{Pd}_3(\text{dppm})_3\text{CO}^{2+}$ is calculated to be 0.19 \AA according to ADF. An emission band fitting similar to a Franck–Condon analysis also reports a ΔQ of 0.19 \AA : Provencher, R.; Harvey, P. D. *Inorg. Chem.* **1996**, 35, 2113.
- (8) (a) Schubert, V. J.; Neugebauer, D.; Aly, A. A. M. *Z. Anorg. Allg. Chem.* **1980**, 464, 217. (b) Aly, A. A. M.; Neugebauer, D.; Orama, O.; Schubert, V.; Schmidbaur, H. *Angew. Chem., Int. Ed. Engl.* **1978**, 17, 125.
- (9) Bresciani, N.; Marsich, N.; Nardin, G.; Randaccio, L. *Inorg. Chim. Acta* **1974**, 10, L5–L6.
- (10) Ho, D. M.; Bau, R. *Inorg. Chem.* **1983**, 22, 4079.



orbital diagram, the electronic transitions, and the evidence of weak Cu...Cu interactions have been addressed theoretically using the density functional theory and experimentally using photoselection emission spectroscopy and a comparative study between a monomeric Cu—phosphine complex and the tricopper cluster. The excited state structure in the lowest energy triplet state (3A_2) has been optimized also using the density functional theory. The excited state distortion (shortening) along the Cu...Cu interactions is predicted to be large.

Experimental Section

Materials. The $[\text{Cu}_3(\text{dppm})_3\text{OH}](\text{BF}_4)_2^{10}$ and $[\text{Cu}(\text{P}(\text{C}_6\text{H}_5)_3)_3]\text{BF}_4^{11}$ complexes have been prepared according to literature procedures. The solvents (ethanol (Fisher), butyronitrile (Aldrich), toluene (Fisher), 2-propanol (Fisher), and methylcyclohexane (Fisher)) were purified by standard procedures.¹²

Spectroscopic Measurements. Absorption spectra were measured on a Hewlett Packard 8452 A diode array spectrometer, and emission and excitation spectra were obtained using a Spex Fluorolog II spectrometer or a PTI LS 100 spectrometer. Part of the emission lifetime measurements were also performed on the PTI LS 100 instrument. The second part of the measurements were performed on the Spex Fluorolog II spectrometer equipped with a Spex 1934 D phosphorimeter setup (for lifetimes that are at least $>10 \mu\text{s}$). Raman spectra were measured on an Instruments SA. Raman spectrometer equipped with a U-1000 Jobin-Yvon 1.0 double monochromator using the 514.5 nm green line of a Spectra-Physics argon ion laser for excitation. Picosecond flash photolysis measurements were performed at the Center for Picosecond Spectroscopy at Concordia University. A description of the setup can be found in ref 34b.

Experimental Procedures. Emission quantum yields (Φ_e) were measured using 9,10-diphenylanthracene as the standard according to published procedures.¹³ Binding constants were measured according to procedures outlined in reference 5c. Polarization ratios (N) were also measured according to literature procedures.¹⁴ All solutions were Ar(g) bubble degassed for room-temperature measurements (298 K), unless stated otherwise.

Computational Details. The CACAO¹⁵ graphics package was used to draw the molecular orbitals. In order to enhance clarity, they were redrawn using the Chem Draw computer software. The CACAO program was included in software based on extended Hückel molecular orbital calculations.¹⁶ These

Table 1. Calculated MO Levels for $\text{Cu}_3(\text{PH}_3)_6\text{OH}^{2+}$

MO label	calcd energy/eV	MO label	calcd energy/eV
14a ₁	−8.416	16e	−13.115
13a ₁ (LUMO)	−8.533	11a ₁	−13.136
7a ₂ (HOMO)	−11.859	10a ₁	−13.295
18e	−11.954	15e	−13.300
17e	−12.957	6a ₂	−13.321
12a ₁	−13.017	14e	−13.395

calculations were performed using a modified version of the Wolfsberg—Helmholz formula.¹⁷ The atomic parameters used for Cu, P, H, and O were taken from the literature.^{16,18} The interatomic distances and valence bond angles were average values taken from ref 10, in which the crystal structure of the $\text{Cu}_3(\text{dppm})_3\text{OH}^{2+}$ cation is reported. To simplify the calculations (limitations in the size of the molecules handled by the program), the dppm ligands were replaced by two PH_3 groups. Such a procedure is standard. The reported density functional calculations were all carried out by utilizing the program ADF version 1.1.3 which was developed by Baerends et al.^{19,20} and vectorized by Ravenek.²¹ The numerical integration procedure applied for the calculations was developed by te Velde et al.²² The geometry optimization procedure was based on the method developed by Versluis and Ziegler. The electronic configurations of the molecular systems were described by an uncontracted double- ζ basis set²³ on copper for 3s, 3p, and 4s and triple- ζ for 4d. Double- ζ STO basis sets²⁴ were used for phosphorus (3s, 3p), oxygen (2s, 2p), and hydrogen (1s), augmented with a single 3d polarization function, except for hydrogen, where a 2p function was used. Polarization functions were not used for copper. The $1s^2 2s^2 2p^6$ configuration on copper, the $1s^2 2s^2$ configuration on phosphorus, and the $1s^2$ configuration on oxygen were assigned to the core and treated by the frozen-core approximation.²⁰ A set of auxiliary²⁵ s, p, d, f, and g STO functions, centered on all nuclei, was used in order to fit the molecular density and present Coulomb and exchange potentials accurately in each SCF cycle. Energy differences were calculated by including the local exchange-correlation potential of Vosko et al.²⁶ No nonlocal exchange and nonlocal correlation correction was made for the geometry optimization.

Results and Discussion

1. Theoretical Calculations. The molecular orbital energy diagram for the frontier orbitals of the model compound $\text{Cu}_3(\text{PH}_3)_6\text{OH}^{2+}$ was computed using the density functional theory (Table 1). The MO's of interest in this work are the

- (11) Gaughan, A. P., Jr.; Dori, Z.; Ibers, J. A. *Inorg. Chem.* **1974**, *13*, 1657.
- (12) (a) Perrin, D. D.; Armarego, W. L. F.; Perrin, D. R. *Purification of Laboratory Chemicals*; Pergamon: Oxford, U.K., 1966. (b) Gordon, A. J.; Ford, R. A. *The Chemist's Companion, a Handbook of Practical Data, Techniques, and References*; Wiley: New York, 1972; p 436.
- (13) Lim, E. C.; Laposa, J. D.; Yu, J. M. H. *J. Mol. Spectrosc.* **1966**, *19*, 412.
- (14) See for examples: (a) Zelent, B.; Harvey, P. D.; Durocher, G. *Can. J. Spectrosc.* **1984**, *29*, 23. (b) *Can. J. Spectrosc.* **1983**, *28*, 188. (c) Harvey, P. D.; Zelent, B.; Durocher, G. *Spectrosc. Int. J.* **1983**, *2*, 128 and references therein. (d) Brummer, J. G.; Crosby, G. A. *Chem. Phys. Lett.* **1984**, *112*, 15.
- (15) Mealli, C.; Proserpio, D. M. *J. Chem. Educ.* **1990**, *67*, 399.
- (16) (a) Hoffmann, R.; Lipscomb, W. M. *J. Chem. Phys.* **1962**, *36*, 2179. (b) Hoffmann, R.; Lipscomb, W. M. *J. Chem. Phys.* **1962**, *37*, 2872. (c) Hoffmann, R. *J. Chem. Phys.* **1963**, *39*, 1397.

- (17) Ammeter, J. H.; Burgi, H. B.; Thibeault, J. C.; Hoffmann, R. *J. Am. Chem. Soc.* **1978**, *100*, 3686.
- (18) (a) Summerville, R. H.; Hoffmann, R. *J. Am. Chem. Soc.* **1976**, *98*, 7240. (b) Hay, P. J.; Thibeault, J. P.; Hoffmann, R. *J. Am. Chem. Soc.* **1975**, *97*, 4884.
- (19) Baerends, E. J.; Ellis, D. E.; Ros, P. *Chem. Phys.* **1973**, *2*, 41.
- (20) Baerends, E. J. Ph.D. Thesis, Vrije Universiteit, Amsterdam, 1975.
- (21) Ravenek, W. In *Algorithms and Applications on Vector and Parallel Computers*; Rigie, H. J. J.; Dekker, Th. J., van de Vorst, H. A., Eds.; Elsevier: Amsterdam, 1987.
- (22) Boerrigter, P. M.; te Velde, G.; Baerends, E. J. *Int. J. Quantum Chem.* **1988**, *33*, 87.
- (23) (a) Snijders, G. J.; Baerends, E. J.; Vernooys, P. *At. Nucl. Data Tables* **1982**, *26*, 483. (b) Vernooys, P.; Snijders, G. J.; Baerends, E. J. *Slater Type Basis Functions for the Whole Periodic System*; Internal Report; Free University of Amsterdam: Amsterdam, 1981.
- (24) (a) Noodleman, L.; Norman, J. G. *J. Chem. Phys.* **1979**, *70*, 4903. (b) Noodleman, L. *J. Chem. Phys.* **1981**, *74*, 5737. (c) Noodleman, L.; Baerends, E. J. *J. Am. Chem. Soc.* **1984**, *106*, 2316.
- (25) Krijn, J.; Baerends, E. J. *Fit functions in the HFS-method*; Internal Report (in Dutch); Free University of Amsterdam: Amsterdam, 1984.
- (26) Vosko, S. D.; Wilk, L.; Nusair, M. *Can. J. Phys.* **1990**, *58*, 1200.

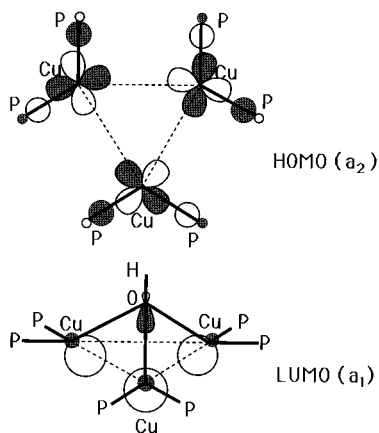


Figure 1. Drawing of the LUMO and HOMO of the $\text{Cu}_3(\text{PH}_3)_6\text{OH}^{2+}$ model compound. In the HOMO drawing, the O atom, omitted for clarity, does not contribute to the MO.

Table 2. Atomic Contributions for the $\text{Cu}_3(\text{PH}_3)_6\text{OH}^{2+}$ Frontier Orbitals

	%											
	Cu			P			O			other		
	$d_{x^2-y^2}$	d_{xy}	s	p_x	p_y	p_z	p_x	p_y	p_z	p_x	p_y	p_z
LUMO ($13a_1$)			27	22	22	18						4
HOMO ($7a_2$)	26	25		6	4		13	16				10
18e	14	39		3	8	11	14		1	1		9

$13a_1$ (LUMO), $7a_2$ (HOMO), and $18e$ (HOMO-1). The energy gap between the LUMO and the HOMO is 3.42 eV ($17\,600\text{ cm}^{-1}$), which would generate an absorption band around 360 nm. Experimentally, this band is observed at $\sim 335\text{ nm}$ (section below). The LUMO is composed of $\sim 62\%$ p and $\sim 27\%$ s Cu atomic orbitals. Some O p_z atomic contributions are also computed ($\sim 4\%$). This MO exhibits $\text{Cu}\cdots\text{Cu}$ bonding interactions and some weak antibonding Cu–O interactions. There is no Cu–P component in this MO, and very weak O–H antibonding interactions are felt. Details of the atomic contributions to the MO's are listed in Table 2. The HOMO is primarily composed of $\sim 51\%$ in-plane Cu d orbitals ($d_{x^2-y^2}$, d_{xy}), of $\sim 10\%$ of in-plane Cu p orbitals (p_x , p_y), and of $\sim 29\%$ of in-plane P p orbitals (p_x , p_y). This MO exhibits antibonding interactions for the $\text{Cu}\cdots\text{Cu}$ and Cu–P interactions, but no contribution of the OH group is observed. Finally, the HOMO-1 ($18e$) is composed of $\sim 53\%$ of in plane Cu d atomic contributions ($d_{x^2-y^2}$, d_{xy}), of $\sim 11\%$ Cu p orbitals (p_x , p_y), and of $\sim 25\%$ of in-plane P p orbitals (p_x , p_y). Some weak O atomic contributions are also observed. This MO is located $\sim 0.1\text{ eV}$ below the HOMO, which would theoretically place an absorption band at $\sim 301\text{ nm}$ ($33\,200\text{ cm}^{-1}$). Experimentally, a strong absorption is indeed observed in the $283\text{--}297\text{ nm}$ range. The program used for the computations (ADF 1.1.3) could not draw the MO's. Instead, we used the CACAO program,¹⁵ which utilizes the qualitative EHMO model. During the computations, we verified that the MO's of interest did not change their relative order and did not change their identity (i.e., approximately the same atomic contributions). Figures 1 and 2 show the LUMO and HOMO and HOMO-1, respectively. Some minor inversions in the MO ordering below HOMO-1 are noticed for MO's separated by less than 0.1 eV . These are of little consequence to this work. It is also interesting to note that the MO scheme for the $\text{Cu}_3(\text{PH}_3)_6\text{OH}^+$ model compound is similar to that of the $\text{M}_3(\text{PH}_3)_6\text{CO}^{2+}$ compounds ($\text{M} = \text{Pd}, \text{Pt}$) investigated by our group^{5b} and by others.²⁷ The two major differences are

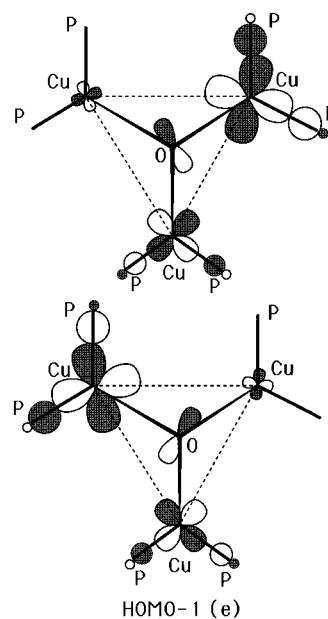


Figure 2. Drawing of HOMO-1 ($18e$) of the $\text{Cu}_3(\text{PH}_3)_6\text{OH}^{2+}$ model compound.

Table 3. Comparison between Selected Experimental and Calculated Bond Distances and Angles for $\text{Cu}_3(\text{PH}_3)_6\text{OH}^{2+}$

	exptl ^a (X-ray data)	calcd (C_{3v})	
		ground state	T_1 excited state
$r(\text{Cu}\cdots\text{Cu})/\text{\AA}$	3.127(2) 3.120(2) 3.320(2)	3.373	2.906
av $r(\text{Cu}-\text{P})/\text{\AA}$	2.232(6)	2.231	2.174
av $r(\text{Cu}-\text{O})/\text{\AA}$	2.01(2)	2.00	1.94
$r(\text{O}-\text{H})/\text{\AA}$		0.989	0.983
av $\angle \text{PCuCu}/\text{deg}$	87(5)	93.8	97.4
av $\angle \text{CuOCu}/\text{deg}$	105(6)	115.1	97.1
av $\angle \text{Cu OH}/\text{deg}$	113(5)	103.0	120.1

^a Data for $\text{Cu}_3(\text{dppm})_3\text{OH}^{2+}$ from ref 10. The uncertainties included in parentheses for average values are the differences between the average values and the most different experimental data.

the addition of two electrons in the Cu_3 complex and the absence of π -back-bonding orbitals in the OH group.

The structure of the $\text{Cu}_3(\text{PH}_3)_6\text{OH}^{2+}$ model cluster in its lowest energy triplet excited state has been optimized using the density functional theory (figure available in the Supporting Information). In order to provide confidence in the calculations, the ground state $\text{Cu}_3(\text{PH}_3)_6\text{OH}^{2+}$ structure is also optimized and compared to that of $\text{Cu}_3(\text{dppm})_3\text{OH}^{2+}$ (Table 3).¹⁰ The comparison between the experimental and calculated valence bond distances (i.e., Cu–P and Cu–O) for the ground state structure is excellent. The calculated O–H bond distance (0.989 for S_0 , 0.983 for T_1) also compares very favorably with the experimental datum (0.970 \AA for OD).²⁸ The calculated $\text{Cu}\cdots\text{Cu}$ separation (3.373 \AA) is somewhat larger than that of the three crystallographically measured $\text{Cu}\cdots\text{Cu}$ distances in $\text{Cu}_3(\text{dppm})_3\text{OH}^{2+}$ (average = 3.189 \AA).¹⁰ This difference is associated with the presence of the bridging dppm ligand and which limits the freedom of the P atoms. In bridged dppm non-metal–metal-bonded trinuclear complexes, the P \cdots P bite distance is generally found to be around 3.3 \AA .^{8,9} For the model compound, values of 3.67 and 3.48 \AA are calculated for the P \cdots P separations

(27) (a) Mealli, C. *J. Am. Chem. Soc.* **1985**, *107*, 2245. (b) Evans, D. G. *J. Organomet. Chem.* **1988**, 352, 397.

(28) Weast, R. C., Selby, S. M., Eds. *CRC Handbook of Chemistry and Physics*, 48th ed.; The Chemical Rubber Co.: Cleveland, OH, 1968; p F147.

($\text{PH}_3 \cdots \text{PH}_3$) of the S_0 and T_1 structures, respectively, and may explain in part some of the small differences in valence bond angles between the X-ray and calculated S_0 data. Upon removal of the dppm ligand from the ground state model cluster, the $\text{Cu} \cdots \text{Cu}$ separations increase slightly, which certainly indicates that the $\text{M} \cdots \text{M}$ interactions are very weak from a theoretical standpoint. At distances of 3.2–3.4 Å, the metal atoms are well located above the sum of the van der Waals radii (i.e., $1.40 \times 2 = 2.80$ Å).²⁹ Numerous experimental works have demonstrated that (weak) $\text{M} \cdots \text{M}$ interactions are still possible at distances exceeding the van der Waals limit and can be detected in polynuclear complexes³⁰ ($\text{M} = \text{Rh},^{30a} \text{Pd},^{30b} \text{Pt},^{30c} \text{Hg}^{30d}$), notably by Raman and electronic spectroscopy. This phenomenon has been known for years because of the so-called van der Waals molecules.³¹ In the T_1 excited state, this calculated distance undergoes a remarkable decrease going from 3.373 down to 2.906 Å (i.e., calculated excited state distortion $\Delta Q = 0.467$ Å). This observation is in perfect agreement with the MO diagram, which indicates that the HOMO is $\text{Cu} \cdots \text{Cu}$ antibonding and that the LUMO $\text{Cu} \cdots \text{Cu}$ is bonding. This predicted ΔQ value is somewhat larger than that of the experimentally evaluated one for the related $d^{10}-d^{10}$ $\text{Pd}_2(\text{dppm})_3$ complex ($\Delta Q \sim 0.18-0.23$ Å),³² indicating that the $\text{Cu}_3(\text{dppm})_3\text{OH}^{2+}$ cluster is expected to be a more flexible molecule than the dimer. But again, the absence of the dppm ligand in the computations increases the degree of freedom of the $\text{Cu}(\text{PH}_3)_2$ fragments. Nevertheless, in relation to the excited state guest–host activities, these computations predict that the cavity size should be greatly reduced in the T_1 state. In addition, the antibonding nature of the $\text{Cu}-\text{P}$ interactions in the HOMO, and the non contributing $\text{Cu}-\text{P}$ interactions in the LUMO, predict that the $\text{Cu}-\text{P}$ distances in the excited state should be somewhat shorter than that of the ground state. This is indeed computed (2.231 Å for S_0 and 2.174 Å for T_1 state) and should also contribute to the decrease in cavity size.

One interesting last point is the comparison of the position of the Cu_3 plane with respect to the P_6 plane. In the ground state, the computed P_6 plane is located below the Cu_3 plane (where the OH group is located on top) by 0.10 Å. In the T_1 state, the calculated P_6 plane has moved up above the Cu_3 plane by about 0.07 Å. This structural modification renders the CuP_3 fragments less planar in the excited state, deforming the p_z Cu orbitals in order to promote larger $\text{Cu } p_z \cdots p_z$ Cu positive MO overlaps.

2. UV–Vis Spectra. In order to address evidence of $\text{Cu} \cdots \text{Cu}$ interactions, the UV–vis spectra of the monomeric triangular planar $[\text{Cu}(\text{P}(\text{C}_6\text{H}_5)_3)_3]^+$ complex are investigated.³³ The 298 K spectra of the monomer are characterized by a vibrationally resolved band located at 278 nm ($\epsilon = 4400 \text{ M}^{-1} \text{ cm}^{-1}$), with a weak tail around 300 nm. On the other hand, the cluster exhibits an intense shoulder at 255 nm ($\epsilon = 41\,000 \text{ M}^{-1} \text{ cm}^{-1}$) and a second one at ~ 310 nm. The 278 nm

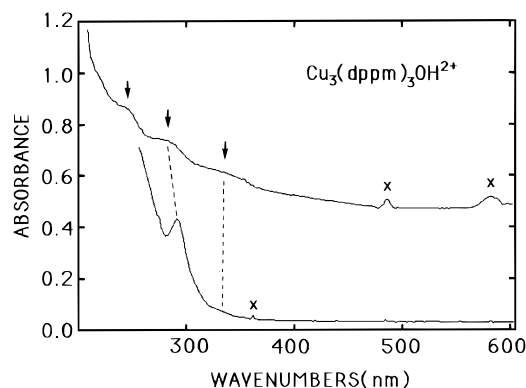


Figure 3. Comparison of the UV–vis spectra for solid $\text{Cu}_3(\text{dppm})_3\text{OH}^{2+}$ at 298 K (top) and for $\text{Cu}_3(\text{dppm})_3\text{OH}^{2+}$ in ethanol (at 77 K for resolution improvement purposes; bottom).

Table 4. Comparison of the UV–Vis Data

exptl			calcd	
λ/nm			λ/nm	proposed assignt
solid state (298 K)	ethanol (77 K)	comment		
335 (sh)	337 (sh)	weak	360	$7a_2 \rightarrow 13a_1$
283 (sh)	297	strong	301	$18e \rightarrow 13a_1$
250 (sh)	~ 260 (sh)			

structured band in the monomeric species is clearly characteristic of an intraligand ($\text{P}(\text{C}_6\text{H}_5)_3$) absorption. The strongly allowed character of the 255 nm band in the cluster compound indicates that different electronic transitions are taking place and indicates some evidence of weak $\text{Cu} \cdots \text{Cu}$ interactions in the cluster. Further evidence is also provided from the comparison of the emission spectra (see text below).

The 298 K solid state and 77 K solution UV–visible spectra of $\text{Cu}_3(\text{dppm})_3\text{OH}^{2+}$ are shown in Figure 3 (Table 4). Both exhibit features in the 290 and 335 nm range in agreement with the theoretical predictions.

3. Emission Spectra. Despite the fact that the compound was reported over 10 years ago, the luminescence properties appear never to have been investigated. The $\text{Cu}_3(\text{dppm})_3\text{OH}^{2+}$ cluster is indeed strongly luminescent both in the solid state (Figure 4) and in solutions (Supporting Information). The solid state emission ($\lambda_{\text{max}} = 510$ nm at 77 K) is located between the emissions found for the solutions ($\lambda_{\text{emi}} = 480$ nm, $\tau_e = 170 \pm 40 \mu\text{s}$, $\Phi_e = 0.73$ at 77 K, $\lambda_{\text{max}} = 540$ nm, $\tau_e = 89 \pm 9 \mu\text{s}$, $\Phi_e = 0.14$ at 298 K). In O_2 -saturated solutions at 298 K, practically no luminescence is observed. This efficient O_2 quenching precludes any accurate measurement of τ_e on our instruments.³⁴ Both bands are vibrationally unstructured. The emission spectra

(29) Cotton, F. A.; Wilkinson, G.; Gauss, P. L. *Basic Inorganic Chemistry*, 3rd ed.; Wiley: Toronto, 1995; p 61.

(30) (a) Harvey, P. D.; Shafiq, F.; Eisenberg, R. *Inorg. Chem.* **1994**, *33*, 3424. (b) Perreault, D.; Drouin, M.; Michel, A.; Harvey, P. D. *Inorg. Chem.* **1993**, *32*, 1903. (c) Harvey, P. D.; Truong, K.; Aye, D. T.; Bandrauk, A. D. *Inorg. Chem.* **1994**, *33*, 2347. (d) Harvey, P. D.; Aye, K. T.; Isabel, E.; Hierso, K.; Lognot, I.; Mugnier, Y.; Rochon, F. *Inorg. Chem.* **1994**, *33*, 5981. (e) Harvey, P. D. *Coord. Chem. Rev.*, in press.

(31) See the numerous data contained in: Huber, K. P.; Herzberg, G. *Molecular Spectra and Molecular Structure Constants of Diatomic Molecules*; Van Nostrand: New York, 1979. See also the numerous examples cited in reference 30.

(32) (a) Harvey, P. D.; Murtaza, Z. *Inorg. Chem.* **1993**, *32*, 4721. (b) Harvey, P. D.; Dallinger, R. F.; Woodruff, W. H.; Gray, H. B. *Inorg. Chem.* **1989**, *28*, 3057.

(33) An attempt to obtain the $\nu(\text{Cu} \cdots \text{Cu})$ values for the a_1 and e modes of the $\text{Cu}_3(\text{dppm})_3\text{OH}^{2+}$ cluster by Raman spectroscopy has been made. The solid state spectrum is composed of a broad and strong shoulder located at 39 cm^{-1} . These modes are believed to be located under this broad envelope by comparing data for Ag_n ($n = 2, 3$) complexes.^{30b} The monomeric species $[\text{Cu}(\text{P}(\text{C}_6\text{H}_5)_3)_3]^+$ exhibits Raman weaker scatterings at 47 and 73 cm^{-1} . The spectra are available in the Supporting Information.

(34) (a) An attempt to measure τ_e in O_2 -saturated solutions was made using picosecond flash photolysis available at Concordia University. A transient absorption centered around 600 nm is initially observed and decays in the long-nanosecond regime. On the other hand, a new transient located at ~ 500 nm appears, also in the long-nanosecond time scale. The τ_e values are still undetermined because these measurements were accompanied by a photochemical transformation indicating the presence of a reaction. This system was not investigated further. The flash photolysis transient spectra are provided in the Supporting Information. (b) A description of the optical setup used in these measurements is provided in one of our previous works: Harvey, P. D.; Gan, L.; Aubry, C. *Can. J. Chem.* **1990**, *68*, 2278.

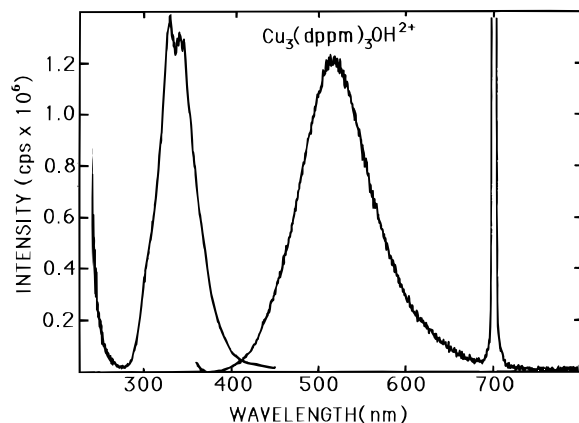


Figure 4. Solid state emission (right) and excitation spectra (left) of $\text{Cu}_3(\text{dppm})_3\text{OH}^{2+}$ at 77 K. The peak at 700 nm is an instrumental artifact (first harmonic of λ excitation at 350 nm).

for the monomeric $[\text{Cu}(\text{P}(\text{C}_6\text{H}_5)_3)_3]\text{BF}_4$ compound in ethanol at 77 K is centered at 400 nm and exhibits some complicated vibrational structures (presumably associated with an intraligand phosphorescence). In this case, $\tau_e \sim 1$ ms (i.e., $934 \pm 37 \mu\text{s}$ at 77 K in ethanol). Both excitation and absorption spectra show a shoulder at ~ 290 nm (different from 300 nm for the Cu_3 cluster). These results clearly indicate that the $\text{Cu}_3(\text{dppm})_3\text{OH}^{2+}$ emission does not arise from a localized independent excited CuP_2^+ center but rather is delocalized within the Cu_3 frame. Since the τ_e values are relatively long and the energy gap between the emission and lowest energy absorption maxima are large (on the order of $11\,000 \pm 1000 \text{ cm}^{-1}$), the emission is a phosphorescence.

In order to make firm assignments regarding the nature of the emissive state, the photoselection technique is applied. The polarization ratio, N , is given by $(I_V/I_H)_V/(I_H/I_V)_H$. $(I_V/I_H)_V$ is the ratio of the intensities of vertically to horizontally polarized emissions when excited with vertically polarized light, and $(I_H/I_V)_H$ is the ratio of the intensities of horizontal and vertical emissions with horizontally polarized excitation. N is then related to the relative orientation of transition moments in absorption and emission. The theoretical value of $N = 3$ indicates that the absorption is polarized along a single molecular axis followed by an emission along the same axis. $N = 0.5$ indicates single-axis absorption followed by emission along a perpendicular axis. (In practice, these theoretical values were never obtained; this is due in part to the natural depolarization of the glass.) In the special case where $N = 1$, the emission is considered to be depolarized. The C_{3v} geometry of the molecule allows only two transition polarizations to occur in the case of orbitally allowed transitions: along the z axis and along the x,y plane. Hence, an absorption polarized along the z axis followed by an emission polarized parallel would produce a polarization ratio approaching the theoretical value of 3.0. On the other hand, one optical process involving x,y -plane polarization will generate a polarization ratio of 1.0 (depolarized light, since there is no discrimination between the two polarizer positions). Theoretically, only the $a_2 \rightarrow a_2$ and $a_1 \rightarrow a_1$ transitions should be z -polarized. An $a_2 \rightarrow a_1$ transition has an unknown transition moment, and therefore the polarization value can take any value. Figure 5 summarizes one possible scenario of how the energy levels could be placed. The 3A_2 state exhibits two sublevels including the spin-orbit coupling ($A_1 + E$). Generally the A_1 -(z) state is the most stable.^{14d} The polarization ratios for the emission excitation spectra of $\text{Cu}_3(\text{dppm})_3\text{OH}^{2+}$ in ethanol at 77 K (Figure 6) reproducibly exhibit a polarization ratio averaging ~ 1 between 240 and 300 nm, indicating that the emission is depolarized. This result allows a firm assignment

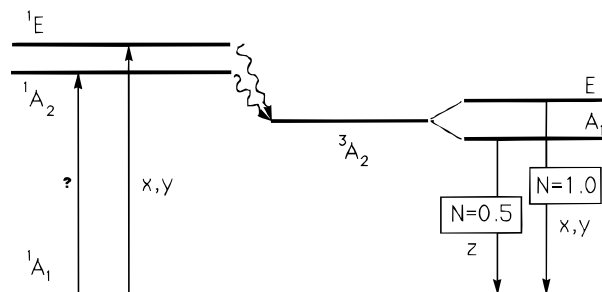


Figure 5. Energy diagram for $\text{Cu}_3(\text{dppm})_3\text{OH}^{2+}$ showing the two lowest energy singlet states (1E and 1A_2) and the lowest energy triplet state (3A_2) which is split into the E and A_1 sublevels. This is one possible scenario. The experimental polarization results support this diagram, which has been adopted for interpretation purposes.

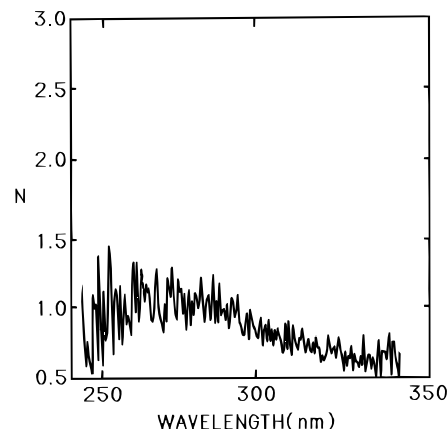


Figure 6. Polarization ratio (N) measured along the excitation spectrum of $\text{Cu}_3(\text{dppm})_3\text{OH}^{2+}$ in ethanol at 77 K.

for the 300 nm feature: $e \rightarrow a_1$ below 300 nm. N decreases steadily down to about 0.65–0.70, showing some degree of polarization, which indicates that another electronic transition (differently polarized) takes place in the unresolved tail of the 300 nm band (i.e., between 300 and 350 nm). The only reasonable candidate is $a_2 \rightarrow a_1$, as suggested by the density functional theoretical MO calculations. The emission is therefore assigned to a radiation transition from the 3A_2 state to the ground 1A_1 state. (N.B. If the 1E state would have been placed below the 1A_2 state, the ratios of 0.65–0.70 would not have been observed.)

The perturbation of the photophysical properties by addition of guest molecules has also been investigated. The expression “guest molecules” refers to the fact that any interactions between a substrate and the lumophore (i.e., the Cu_3 center) must automatically occur within the pocket formed by the dppm phenyl groups; therefore the substrates are then also submitted to the cavity steric hindrance and hydrophobic interactions. On the basis of the very large binding constants measured for the related $\text{Pd}_3(\text{dppm})_3\text{CO}^{2+}$ compound with various carboxylate guest molecules ($730 < K_{11} < 10\,000 \text{ M}^{-1}$),^{5c} the choice of substrates was the acetate and the 4-aminobenzoate anion (as sodium salt). The binding constants were $730 \pm 30 \text{ M}^{-1}$ for acetate and $3300 \pm 300 \text{ M}^{-1}$ for 4-aminobenzoate using methanol as the solvent at 298 K^{5c} (i.e., a $\sim 1:4$ relative ratio). The $\text{Cu}_3(\text{dppm})_3\text{OH}^{2+}$ emission at 298 K is readily quenched by the addition of the carboxylate compounds (Figure 7). These spectroscopic changes are accompanied by the presence of isosbestic points in the UV spectra of $\text{Cu}_3(\text{dppm})_3\text{OH}^{2+}$ in ethanol (at ~ 325 nm with the addition of acetate and at ~ 330 nm with the addition of 4-aminobenzoate).³⁵ The quenching constants measured by Stern–Volmer methods (τ_0/τ vs $[Q]$; τ_0 = emission lifetime without quencher, τ = emission lifetime

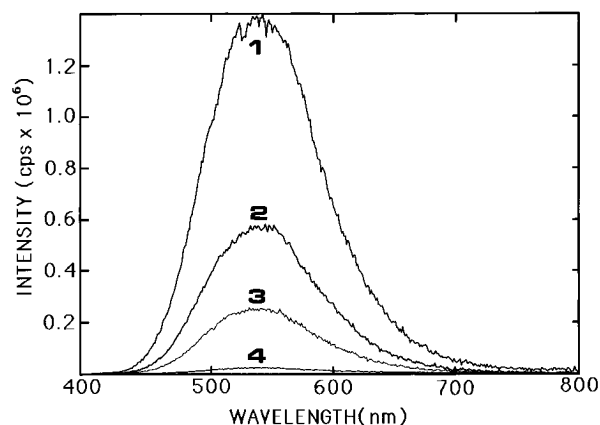


Figure 7. Typical emission intensity quenching experiment for the addition of 4-aminobenzoate to an Ar(g)-degassed ethanolic solution of $\text{Cu}_3(\text{dppm})_3\text{OH}^{2+}$ at 298 K: (1) no quencher; (2) 1.07×10^{-5} M; (3) 3.15×10^{-5} M; (4) 4.15×10^{-5} M.

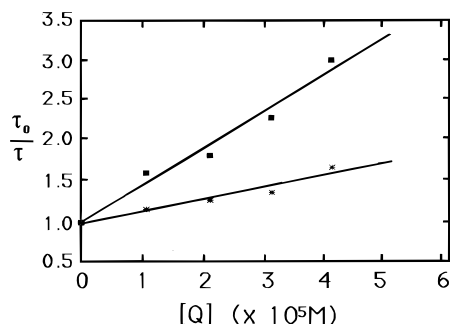


Figure 8. Stern-Volmer plot (τ_0/τ vs $[Q]$) for the quenching of $\text{Cu}_3(\text{dppm})_3\text{OH}^{2+}$ in a degassed ethanol solution at 298 K by sodium acetate (*) and sodium 4-aminobenzoate (■).

with quencher, slope = $K_{SV} = \tau_0 k_q$) give the following results: $K_{SV} = 1.46 \times 10^4$ and $4.52 \times 10^4 \text{ M}^{-1}$ and $k_q = 1.65 \times 10^8$ and $5.10 \times 10^8 \text{ M}^{-1} \text{ s}^{-1}$ for acetate and 4-aminobenzoate, respectively (Figure 8).³⁶ The ratio $k_q(\text{acetate}):k_q(4\text{-aminobenzoate})$ is $\sim 1:3$, which is not too different from the relative ratio of the binding constants stated above. The decays were found to be monoexponential. McMillin *et al.*³⁷ have investigated the emission properties for the complex $\text{Cu}(\text{dmp})_2^+$ (dmp = dimethylphenantroline). They have proposed an exciplex formation in order to explain the emission quenching by various substrates including Lewis donors, triplet energy acceptors, and acetate. The proposed structure of this exciplex was a penta-coordinated Cu compound with two dmp ligands and a Lewis donor. In the Stern-Volmer plot for the $^*\text{Cu}(\text{dmp})_2^+/\text{acetate}$ quenching experiments, the line exhibits an upward curvature and is fitted with a second-order equation (i.e., $[Q] + [Q]^2$), indicating that two excited state quenching pathways are present. In this work, the line is straight (within the experimental

Table 5. Spectroscopic and Emission Data at 77 K

solvent	$\lambda_{\text{max}}/\text{nm}$	$\tau_e/\mu\text{s}^a$
butyronitrile	430 ± 5	290
methylcyclohexane	470 ± 5	220
2-propanol	440 ± 5	~ 200
2-methyltetrahydrofuran	430 ± 5	
ethanol	430 ± 5	170
toluene	470 ± 5	150

^a The estimated uncertainty is $\pm 20 \mu\text{s}$, except that for ethanol, which is $\pm 40 \mu\text{s}$.

uncertainties), indicating a unique pathway. Such a result is consistent with an exciplex formation between the carboxylates and $\text{Cu}_3(\text{dppm})_3\text{OH}^{2+}$. This interaction must occur within the sterically constrained cavity, leading to a unique conformation. Quenching occurring via an energy or electron transfer to the carboxylate compounds is unlikely. Also relevant to this work, efficient excited state deactivations of the cluster compound $\text{Cu}_4\text{I}_4(\text{py})_4$ (py = pyridine) by Lewis donors have also been observed.^{1d} For instance $k_q = (5.9 \pm 0.5) \times 10^9 \text{ M}^{-1} \text{ s}^{-1}$ for $^*\text{Cu}_4\text{I}_4(\text{py})_4/\text{py}^{1d}$ and is ~ 1 order of magnitude larger than that observed in this work. py was not used here since the $\text{Cu}_3(\text{dppm})_3\text{OH}^{2+}$ absorption spectrum is "screened" by the one py (i.e., excitation would take place in both the cluster and the py).

In our recent paper on $\text{Pt}_3(\text{dppm})_3\text{CO}^{2+}$,^{5b} the emission spectra and lifetimes at 77 K for the cluster in various solvents were obtained in order to study the solvent perturbation of the photophysical properties. The τ_e values were found to vary from 10 to 18 μs (protonated solvents), and λ_{emi} at maximum ranged from 630 to 680 nm. These variations were too great to be associated with a simple solvation effect and were interpreted by specific interactions between the unsaturated luminescent Pt_3 center in the excited states and the solvent molecules. A similar study was performed for $\text{Cu}_3(\text{dppm})_3\text{OH}^{2+}$ (Table 5). The variation of τ_e and λ_{emi} is also solvent dependent where $150 \leq \tau_e \leq 290 \mu\text{s}$ and $430 \leq \lambda_{\text{emi}} \leq 470 \text{ nm}$. However, the trends observed for $\text{Cu}_3(\text{dppm})_3\text{OH}^{2+}$ and $\text{Pt}_3(\text{dppm})_3\text{CO}^{2+}$ ^{5b} are not exactly the same. For instance, τ_e varies as toluene < methanol < dimethylformamide < 2-propanol < 2-methyltetrahydrofuran < butyronitrile < ethanol for $\text{Pt}_3(\text{dppm})_3\text{CO}^{2+}$.^{5b} For $\text{Cu}_3(\text{dppm})_3\text{OH}^{2+}$, this trend is toluene < ethanol < 2-propanol \leq methylcyclohexane < butyronitrile. The ethanol/butyronitrile relative order is reversed. The three major differences between the clusters are (1) the cavity size ($\text{Cu} > \text{Pt}$), (2) the (excited states and ground state) electronic configurations, and (3) the Lewis acid properties (hard vs soft). These differences are certainly responsible for a change in cluster-solvent interaction and may explain the changes in trends in τ_e as a function of solvents. It is unclear how each of these factors affect τ_e . Nonetheless, these measurements are an indication that the $\text{Cu}_3(\text{dppm})_3\text{OH}^{2+}$ and the $\text{M}_3(\text{dppm})_3\text{CO}^{2+}$ clusters ($\text{M} = \text{Pd}, \text{Pt}$) do not exactly behave similarly in their guest-host interactions.

This work has provided a number of experimental data which, by comparison with data reported for the well-known $\text{M}_3(\text{dppm})_3\text{CO}^{2+}$ complexes ($\text{M} = \text{Pd}, \text{Pt}$), support the host-guest model. Some differences are noted and need to be rationalized. Numerous mononuclear Cu(I) phosphine complexes have been investigated in the literature for their luminescence properties and their photosensitizing activities in relation to solar energy storage.³⁸ For instance, the photoassisted conversion of norbornadiene into quadricyclane has been extensively investigated as a function of various Cu(I) phosphine complexes. The

(35) We have attempted to measure the association constants (K_{11}) for $\text{Cu}_3(\text{dppm})_3\text{OH}^{2+}$ with carboxylate compounds using spectroscopic methods outlined in ref 5c. Unfortunately the *p*-aminobenzoate absorption spectrum overlaps almost entirely with the cluster one. For acetate, isosbestic points are also evident upon addition of substrates, but the variation of the absorbance was too small to estimate K_{11} . It is not possible to make any comparison with the emission-quenching experiments in these cases. Instead, we have employed data available for the $\text{Pd}_3(\text{dppm})_3\text{CO}^{2+}$ complex.^{5c} The spectroscopic changes associated with $\text{Cu}_3(\text{dppm})_3\text{OH}^{2+}$ in ethanol upon addition of acetate are available in the Supporting Information.

(36) During this investigation there has been no evidence for a breakdown of the cluster or loss of the OH group upon photolysis in the presence of carboxylates (from ^1H NMR, UV-visible, and IR spectroscopy).

(37) (a) Palmer, C. E. A.; McMillin, D. R.; Kirmaier, C.; Holten, D. *Inorg. Chem.* **1987**, 26, 3167. (b) Stacey, E. M.; McMillin, D. R. *Inorg. Chem.* **1990**, 29, 393.

photosensitized interconversion of *cis*- and *trans*-piperylenes is also known to occur using $\text{Cu(I)} \text{BH}_4$ phosphine complexes.^{38g} Such photochemistry differs from that presented in this work. Although no experiment was attempted to see whether $\text{Cu}_3(\text{dppm})_3\text{OH}^{2+}$ could be used as a photosensitizer for the isomerization of norbornadiene (and other acyclic diolefins), structural models (i.e., CPK) indicate that the $\text{Cu(I)} \cdots \parallel$ interac-

tions would be somewhat weak due to the size of the cavity. Further work in this area is in progress.

Acknowledgment. This research was supported by the NSERC (Natural Sciences and Engineering Research Council) and the FCAR (Fonds Concertés pour l'Avancement de la Recherche). P.D.H. thanks Professor Tom Ziegler for allowing us to perform some of the density functional theory calculations on his computers at the University of Calgary.

Supporting Information Available: Micro Raman spectra of $\text{Cu}_3(\text{dppm})_3\text{OH}^{2+}$ and $[\text{Cu}(\text{P}(\text{C}_6\text{H}_5)_3)_3]^+$, picosecond flash photolysis spectra of $\text{Cu}_3(\text{dppm})_3\text{OH}^{2+}$, and UV-visible spectra of $\text{Cu}_3(\text{dppm})_3\text{OH}^{2+}$ in the presence of acetate and emission and excitation spectra of $\text{Cu}_3(\text{dppm})_3\text{OH}^{2+}$ in ethanol solution at 77 and 298 K (9 pages). Ordering information is given on any current masthead page.

IC950812+

- (38) See for instance: (a) Tife, D. J.; Moore, W. M.; Morse, K. W. *Inorg. Chem.* **1984**, 23, 1545. (b) Fife, J. D.; Moore, W. M.; Morse, K. W. *J. Am. Chem. Soc.* **1985**, 107, 7077. (c) Orchard, S. W.; Kutal, C. *Inorg. Chim. Acta* **1982**, 64, L95. (d) Grutsch, P. A.; Kutal, C. *J. Am. Chem. Soc.* **1979**, 101, 4228. (e) Segers, D. P.; DeArmond, K. M.; Grutsch, P. A.; Kutal, C. *Inorg. Chem.* **1984**, 23, 2874. (f) Grutsch, P. A.; Kutal, C. *J. Am. Chem. Soc.* **1977**, 99, 6460. (g) Liaw, B.; Orchard, S. W.; Kutal, C. *Inorg. Chem.* **1988**, 27, 1311. (h) Borsub, N.; Chang, S.-C.; Kutal, C. *Inorg. Chem.* **1982**, 21, 538. (i) Geoffroy, G. L.; Wrighton, M. S. *Organometallic Photochemistry*; Academic Press: New York, 1979; p 205–215 and the references therein.